Lawrence Berkeley National Laboratory

Title

FACTORS AFFECTING THE DISLOCATION SUBSTRUCTURE IN DEFORMED MAGNESIUM OXIDE

Permalink

https://escholarship.org/uc/item/0xx1k3p8

Author

Elkington, Walter E.

Publication Date

1962-07-01

University of California

Ernest O. Lawrence
Radiation Laboratory

FACTORS AFFECTING THE DISLOCATION
SUBSTRUCTURE IN DEFORMED MAGNESIUM OXIDE

Berkeley, California

DISCLAIMER

UNIVERSITY OF CALIFORNIA

Lawrence Raidation Laboratory
Berkeley, California

Contract No. W-7405-eng-48

FACTORS AFFECTING THE DISLOCATION SUBSTRUCTURE IN DEFORMED MAGNESIUM OXIDE

Walter E. Elkington

M.S. Thesis

July, 1962

TABLE OF CONTENTS

ABSTRACT

The dislocation substructure in single crystals of MgO deformed in four point bending at temperatures from -196°C to 1300°C have been observed by transmission electron microscopy. Elongated edge dislocation pairs were observed at all deformation temperatures. A majority of the pairs started where screw dislocations intersected grown in dislocations. The stability of such pairs depended upon the separation of the dislocations and the deformation temperature. Narrow pairs were observed to have broken up into small prismatic loops at 750°C and above. The maximum separation between the two dislocations of opposite sign approached but never exceeded the value

$$\frac{Gb}{8\pi(1-\nu)\tau}$$

where

   b is the Burger's vector

   τ is the resolved shear stress

   ν is Poisson's ratio

   G is the elastic shear modulus

Heating test samples to 750°C resulted in fresh dislocations becoming aged. This aging caused a yield effect in samples deformed at 750°C.

Grown in dislocations always contained impurity precipitates along their length and often did not lie exactly on a slip plane. Because of either one or both of these factors, grown in dislocations remained immobile during deformation.

INTRODUCTION

The plastic behavior of a crystalline material is primarily determined by the nucleation, motion, and interaction of dislocations within the material. To best understand the mechanisms of plastic deformation one needs a knowledge of the behavior of individual dislocations.

Ionic crystals of the NaCl structure have proved extremely useful in this respect because there are several techniques by which their dislocation substructure can be revealed directly. Gilman and Johnston,[1,2] for example, have used etch pit techniques to study dislocation motion and arrangement in deformed LiF crystals; Amelinckx[3,4] has used internal precipitation techniques to record the grown in substructure in several different ionic crystals, and recently Washburn, Groves et al.[5] have used transmission electron microscopy to study the dislocation substructure in the slip bands of deformed MgO.

Due primarily to the availability of these techniques, much has been learned about the atomic mechanism of plastic deformation in this class of crystals. The most recent developments in this field have led to a better understanding of the processes of dislocation multiplication, slip band widening, and strain hardening. Using the etch pit technique, Gilman and Johnston have followed the development of slip bands in LiF. They found that when an isolated dislocation half loop is expanded by applying a stress, new dislocations are formed in its wake. After an individual loop has moved completely across the crystal and multiplication has proceeded, a narrow slip band densely populated with dislocations is formed. Near the yield stress of the crystal, the band begins to widen. During this lateral growth the etch pit density within

the slip band and the deforming stress remain essentially constant until the surface of the crystal is completely covered with slip bands. At this point further deformation can only occur by the motion of dislocations through previously deformed regions of the crystal. This motion is more difficult because the moving dislocation must cut through dislocation "debris" left in the slip band. It is here that strain hardening begins.

In observing deformed MgO by transmission electron micro-scopy, Washburn, Groves et al. discovered that the predominant defects left in the slip bands of their samples were elongated parallel edge dislocation pairs. These pairs constituted the major portion of the dislocation "debris" left in slip bands. Other observations of moving screw dislocations suggested that these pairs were formed when a moving screw dislocation developed a jog large enough to pin it at a point. When such a jog occurred, a pair of edge dislocations of opposite sign would be formed when the unpinned arms on either side of the jog moved forward. This mechanism of pair formation is also capable of explaining dislocation multiplication and slip band widening; for if the two dislocations which comprise a pair are on slip planes far enough apart, they can pass each other so that each arm can act as a dislocation source on widely separated planes. From dislocation theory it can be shown that for a dislocation source to be formed, the dislocations must be on slip planes separated a distance greater than h_{max} equal to $\frac{Gb}{8\pi(1-\nu)\tau}$, where G is the shear modulus, b is the Burger's vector, ν is Poisson's ratio and τ is the resolved shear stress.

From the above equation, it can be seen that if this mechanism of pair formation is operating there should be a maximum pair size for

each applied stress. The original purpose of this study was to test the validity of this mechanism by determining the stress dependence of maximum pair size. To do this, crystals were deformed at various temperatures so as to vary the flow stress and the resulting dislocation substructure was observed by means of transmission electron microscopy.

During the course of the study, observations were made of the effects of temperature and grown in dislocations on the development of dislocation substructure. These observations will also be discussed.

EXPERIMENTAL PROCEDURES

Test Sample Preparation

Bulk MgO single crystals obtained from the Norton Company were used in this study. To prepare test samples, thin sheets approximately .02 x .3 x 1 in. with $\{100\}$ faces were cleaved from the bulk crystals. After being cleaved, the sheets were mechanically polished to remove cleavage steps and annealed for two hours at 1250°C to remove the surface damage which occurred during polishing. The sheets were then chemically polished to obtain smooth surfaces and to remove any remaining surface damage. The final sheet thickness varied from .009 to .018 in.

Test Procedure

In the temperature range -196°C to 750°C, four point bend tests were performed using a stainless steel testing frame mounted on an Instron testing machine. The span length of the frame was 3/4 in. with the knife edges 1/4 in. apart. The two center knife edges could be moved about two perpendicular axes to provide uniform loading. The outer knife edges were fixed but were parallel to within .001 in. in

1/2 in. All samples were deformed with the testing machine operating at a constant cross-head speed of .05 cm/min. The deflection of the samples was taken as the cross-head displacement and so was a measure of the net displacement between the center knife edges with respect to the outer knife edges.

The samples were heated by a small resistance furnace which fitted around the testing frame. Temperature measurements were made using a thermocouple which was placed about 1/8 in. below and under the test samples. After being tested, the samples were immediately removed from the furnace and allowed to air cool.

All samples were deformed by an amount corresponding to an outer fiber strain of approximately 1%. The outer fiber stress was calculated using elastic theory throughout the load-deflection curve.

Samples deformed at 1000°C and higher were bent by manually pressing an alumina rod against the back face of the sample while it was in the furnace. After being deformed, the sample was removed from the furnace and allowed to air cool.

Transmission Sample Preparation

The deformed specimens were next etched for a few seconds in hot nitric acid. The general area selected for examination in the electron microscope was thinned by rotating the sample slowly above a small jet of hot orthophosphoric acid (110°C). The bend samples were polished from the compression side so that the thin sections obtained were from the tensile surface. Polishing was continued until a hole appeared at some point. The sample was then immediately immersed in distilled water and rinsed in alcohol and anhydrous ether. A diagram of the polishing apparatus is shown in Fig. 1.

The hole produced was usually less than 1 mm in diameter. Areas sufficiently thin to be transparent to the electron beam of the microscope extended in a few hundred microns from the periphery of the hole and could be detected by bright interference fringes when observed in vertical optical illumination.

The next step in preparing the transmission samples was that of removing the thin section from around the hole. The following procedure was finally adopted. A small drop of Lacomit masking lacquer on the end of a fine paint brush was lightly touched to the sample in the area of the hole. The Lacomit wet the surface around the hole forming a circle about 2 mm in diameter which, when dried, protected the thin section. The sample was again polished over the hot acid jet and new holes were allowed to form around the mask. Just before these secondary holes started to join, polishing was stopped by immersing the sample in distilled water. The mask was then removed by disolving it in acetone and the sample was rinsed in distilled water, alcohol, and anhydrous ether. At this point the thin section around the periphery of the hole was almost completely surrounded with secondary holes, making it a rather simple matter to chip the material between the secondary holes and allow the thin section to fall into an electron microscope holder. Figure 2 shows a specimen which has been prepared and loaded into an electron microscope holder in this manner.

Observations were made using both a Hitachi HU - 10 and a Siemens Elmiskop I electron microscope operating at 100 kv.

RESULTS AND DISCUSSION

Mechanical Test Results

When an MgO sample is deformed in four point bending, there is an equal shear stress on four of the six possible $<110>$ $\{110\}$ slip systems. Two of the active systems are on planes which intersect the tension surface (a $\{100\}$ plane) at 45° and two intersect it at 90°. Hereafter, these planes will be referred to as 45° and 90° planes, respectively. In deforming as-polished samples, despite the equal shear stress on the slip planes, deformation occurred predominantly on 45° planes concentrated under the center knife edges. The stress deflection curve for such samples invariably had a high yield stress followed by a sharp drop and jerky flow (Fig. 3a). The high yield stress followed by a sharp drop in stress appears to be a result of the higher stress necessary to nucleate dislocations in MgO than to move them.[6] It is not known why deformation occurred predominantly on 45° planes.

Since in this study it was desired to observe dislocations on both types of slip planes, it was necessary to force the 90° planes to operate. To do this, the tension surface of all remaining samples was lightly sprinkled with alumina particles to introduce fresh dislocations on all slip planes. The effect this had on the stress deflection curve can be seen in Figs. 3b and 3c. The yield stress was lowered and flow was smooth. Microexamination revealed that deformation had occurred on both the 45° and 90° slip planes and was uniformly distributed between the center knife edges.

Sprinkling was effective in activating both types of slip systems and in giving uniform deformation at test temperatures to 550°C. At 750°C, however, samples again showed a high yield stress, a sharp drop

in stress, and jerky flow (Figs. 3h and 3i). Microexamination revealed, as in the case of the as-polished samples, that deformation had occurred mainly on 45° planes concentrated under the center knife edges. Further examination revealed that the dislocations introduced by sprinkling had not moved during deformation. Figure 4 shows a "rosette" of such "pinned" dislocations in a sample deformed at 750°C. In contrast to this behavior, Fig. 5 shows how fresh dislocations have formed slip bands in a sample deformed at room temperature.

It is apparent that some impurity diffuses to dislocations at temperatures above 500°C causing them to become pinned. This "pinning" or "aging" phenomenon is also observed in LiF.[2] To determine if any observable change had occurred during annealing, a transmission specimen was prepared from a sample containing only aged dislocations. Examination of this sample, however, revealed no unusual contrast effects nor any precipitates along the dislocations.

Observations

When transmission samples were viewed in the electron microscope, a {100} plane was always very nearly perpendicular to the electron beam of the microscope. Dislocations, therefore, appeared as their projection on a {100} plane. In the NaCl structure there is only one <110> slip direction for a given {110} slip plane so that all glide dislocations in a given plane will have the same Burger's vector. In a 45° plane, therefore, a pure screw dislocation appears as a straight line lying in the slip direction and terminating at top and bottom surfaces of the crystal; a pure edge dislocation on this plane appears as a straight line perpendicular to the slip direction, and a mixed dislocation may have any shape and direction. In a 90° band a pure screw

dislocation and a mixed dislocation appear as straight lines lying in the slip direction and a pure edge dislocation appears as a point.

The Effect of Temperature on Dislocation Substructure

Changing the temperature of deformation can affect the dislocation substructure for several reasons: First, because the stress necessary to move dislocations decreases with temperature; second, because the ease of slip on secondary planes and of jog formation increases with temperature and third, because the rate of climb for a given climb force increases with temperature.

At low deformation temperatures where the stress necessary to move dislocations is large, glide dislocations approach each other more closely and dense substructures develop. Figure 6 shows dislocations on 45° slip planes in a sample deformed at -196°C. The dislocations are, in general, mixed in character and often change direction quite sharply. In samples deformed at ambient temperatures, dislocations on 45° planes were less dense and individual dislocations less angular than those in the samples deformed at -196°C. At temperatures of 750°C and above the dislocation damage in 45° planes was much less and was generally composed of long straight dislocations which were predominantly edge in character (Fig. 7).

In samples deformed at 750°C and above, narrow dislocation pairs broke up into rows of prismatic loops. Figures 8 through 11 show this occurring in samples deformed at the indicated temperature. This phenomenon has been observed previously by Washburn et al.[1] in MgO, and by Price in zinc[7] and Cd[8]. The driving force for this change in dislocation configuration has been shown to be the associated decrease in elastic energy. Since the transformation occurs at temperatures

where thermally generated vacancies are present in small concentration, the mechanism appears to be one of local diffusion along dislocations. The sharp curvature at the end of the dislocation pairs provides an additional climb force and as a result it is here that the pinching off of loops occurs (Fig. 8).

The Effect of Grown in Dislocations on the Motion of Glide Dislocations

The grown in substructure in NaCl type single crystals has been shown to consist of planar arrays of dislocations which make up subgrain boundaries and of random three dimensional networks of individual dislocations.[3] Microexamination of etched MgO crystals used in this study showed that the crystals had a subgrain size which varied from 1 mm to 10 mm in diameter. Within the subgrains there was an etch pit density of approximately $5 \times 10^4/_{cm}2$ (Fig. 9). Most of these pits had conical bottoms and marked the point of emergence of a grown in dislocation at the crystal surface. A few of the pits were flat bottomed. It is believed that these pits occur at impurity precipitates which may or may not be associated with a dislocation.

In this study it was found that the grown in dislocations always contained precipitates along their length and often did not lie exactly on a slip plane (Figs. 10 to 13). Because of either one or both of these factors, the grown in dislocations usually remained immobile during deformation.

The size and spacing of the precipitates varied from one sample to another and in some cases varied from one dislocation to another within the same sample. Large precipitates were generally present at dislocation nodes (Fig. 13). The spacing of observable precipitates was

not always small enough to pin the dislocation. In Fig. 12, for example, the portion of the dislocation between the most widely spaced precipitates could be bowed to a critical radius at a stress below the yield stress of the crystal. This dislocation probably would have moved during deformation were it not for the fact that it did not lie exactly on a slip plane.

Although the grown in dislocations contribute little to the deformation of a crystal, they are important as barriers to the motion of glide dislocations. Numerous micrographs were taken of areas where glide dislocations had intersected grown in dislocations (Figs. 14, 15, 16, 17 and 18). In these regions of intersection there was always a high density of dislocation "damage". Most of the damage was in the form of dislocation pairs or, in the case of samples deformed at high temperatures, in the form of dislocation loops. It appears that the grown in dislocations are extremely important in the nucleation of dislocation pairs. When the origin of a pair could be found, it was either at a grown in dislocation or at an impurity precipitate.

That dislocation pairs are nucleated at grown in dislocations, suggests that many of the glide dislocations moving through a crystal already contain jogs. A jog on a dislocation is a short segment of edge dislocation which is at right angles to the primary glide plane and can glide only along the direction of the Burger's vector. If the jogs are forced to move in any other direction, they must climb which requires formation of vacant lattice sites or interstitial atoms. When a heavily jogged dislocation intersects a grown in dislocation, it is quite likely that a few jogs may glide together at the cusp that is created to form an immobile large jog. In this case, a dislocation pair will be formed when

the unpinned portions of the dislocation on either side continue to move forward.

This mechanism of pair formation can explain the origin of most of the pairs observed in the deformed MgO samples. Sometimes, however, closed pairs were found in the slip bands in regions away from grown in dislocations which suggests that other nucleation mechanisms do operate.

Jog Formation

Dislocations and pairs in 90° slip bands in samples deformed at -196°C were always very straight and their projections were aligned accurately in a <110> direction (Fig. 19). At higher deformation temperatures where there is more thermal energy available for jog formation, dislocations and pairs in 90° slip bands often did not have projections along a <110> direction. Figures 17, 18 and 20 are micrographs showing this effect in a sample deformed at room temperature. The deviations in <110> alignment indicate that the dislocations do not lie exactly on the {110} planes and hence contain jogs.

In a sample deformed at 1300°C, dislocations in 90° slip bands often contained large jogs. Figure 21a is a micrograph of an area where two 90° slip bands have intersected. It can be seen that a dislocation, predominantly screw in character, has developed two large jogs. One of the jogs appears to have formed in order for the dislocation to avoid an impurity precipitate. Large jogs were also observed on dislocations in regions away from slip band intersections (Fig. 21b).

Jogs may be formed by any one of the following mechanisms: First, by cross-slip on a {100} plane; second by intersection with other dislocations having the proper Bruger's vector, and third, by

collection of point defects. No observations were made, however, which clearly showed how moving dislocations acquired large numbers of jogs.

Stress Dependence of Pair Separation

Dislocation pairs were found at all deformation temperatures. As the flow stress was decreased at higher temperatures, the number of dislocation pairs decreased, but the maximum pair size increased. By measuring the separation of the largest pair observed in samples deformed at known stresses, it was found that the pair size never exceeded the calculated theoretical maximum h_{max}. Figures 22a and 22b show the largest pairs found in samples deformed at stresses of $7\frac{kg}{mm^2}$ and $3\frac{kg}{mm^2}$ respectively.

CONCLUSIONS

1. Dislocation pairs are formed at all deformation temperatures.

2. Narrow dislocation pairs are unstable at 750°C and above and break up into prismatic loops.

3. The majority of pairs are nucleated when jogged screw dislocations intersect grown in dislocations.

4. The maximum observed pair separation never exceeded the value

$$\frac{Gb}{8\pi(1-\nu)\tau}$$

5. Grown in dislocations do not move during deformation because they are either pinned by impurity precipitates or do not lie exactly on a slip plane.

6. The size and spacing of precipitates along grown in dislocations varied from one specimen to another.

7. At a deformation temperature of -196°C, dislocations and pairs lie close to a $\{110\}$ plane. At room temperature, however, there is considerable deviation from a $\{110\}$ plane.

8. The density of damage in slip bands decreases rapidly in the temperature range between room temperature and 500°C.

9. Large jogs were found on dislocations in a sample deformed at 1300°C.

10. Fresh dislocations become immobilized when aged at 750°C.

ACKNOWLEDGMENTS

The author is deeply indebted to Professors J. Washburn and

G. Thomas for their welcome advice and continual encouragement

during this study. The work was performed under the auspices of the

United States Atomic Energy Commission

REFERENCES

1. W. G. Johnston and J. J. Gilman, Dislocation Velocities, Dislocation Densities and Plastic Flow in Lithium Fluoride Crystals, J. Appl. Phys, 2, 129 (1959).

2. J. J. Gilman and W. G. Johnston, Dislocations and Mechanical Properties of Crystals (John Wiley and Sons, Inc., New York, 1957) p.116.

3. S. Amelinckx, ibid., p.3.

4. S. Amelinckx, Dislocation Patterns in KCl, Acta Met., 6, 34 (1958).

5. J. W. Washburn, C. W. Groves, A. Kelly and G. K. Williamson, Electron Microscope Observations of Deformed Magnesium Oxide, Phil. Mag., 5, 991 (1960).

6. R. J. Stokes, T. L. Johnson and C. H. Li, Effect of Surface Condition on the Initiation of Plastic Flow in MgO, Trans. AIME, 215, 437 (1959).

7. P. B. Price, Pyramidal Glide and the Formation of Dislocation Loops in Nearly Perfect Zinc Crystals, Phil. Mag., 50, 875 (1960).

8. P. B. Price, Nonbasal Glide in Dislocation-free Cadmium Crystals, J. Appl. Phys., 32, 1746 (1961).
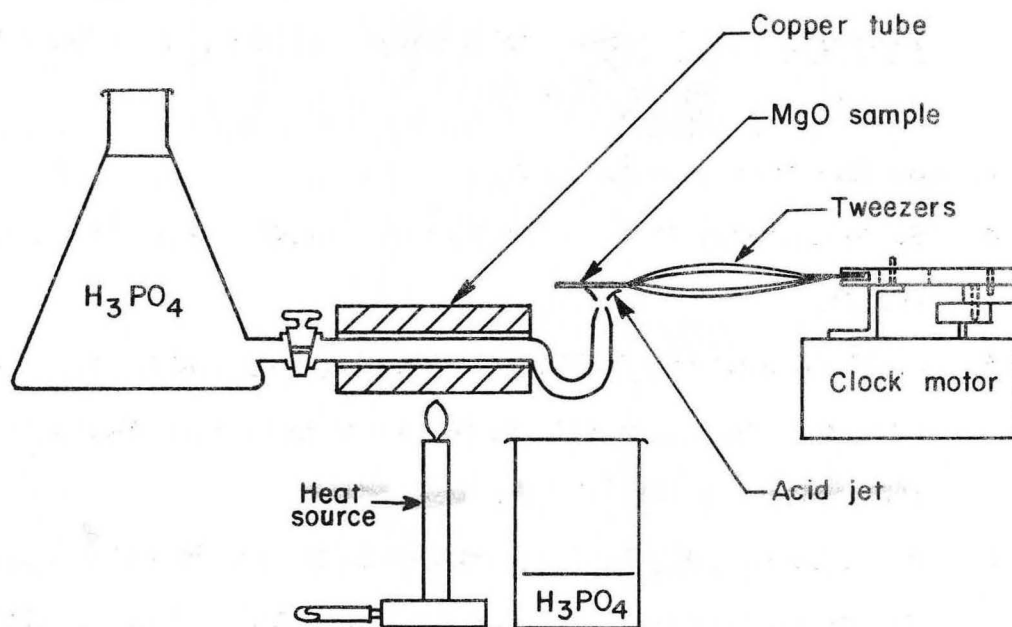
Fig. 1.   Polishing Apparatus.

MU-27554
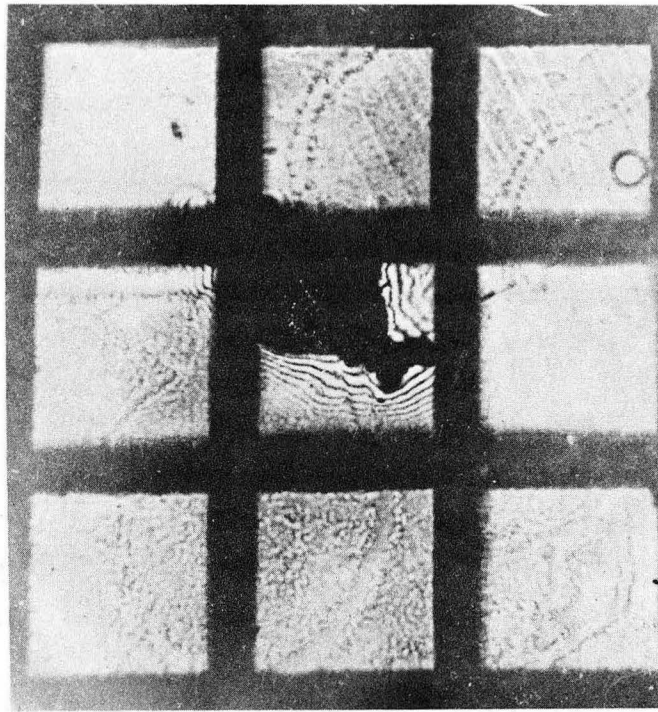
100 μ

ZN-3163

Fig. 2.   Transmission sample loaded in electron
microscope holder.

Fig. 3. Effect of temperature and surface condition
on the stress-deflection curve.

MU-27555

20 μ
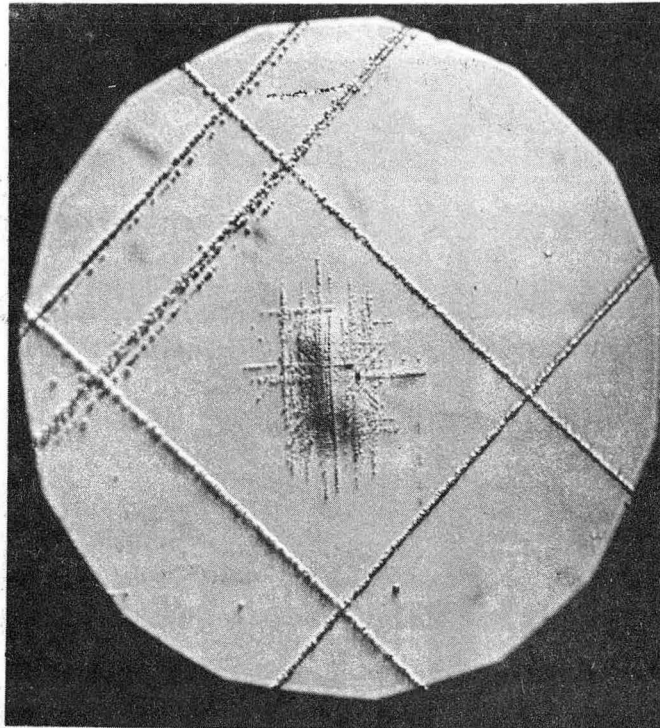
ZN-3168

Fig. 4. Rosette of "aged dislocations" in a sample
deformed at 750°C.
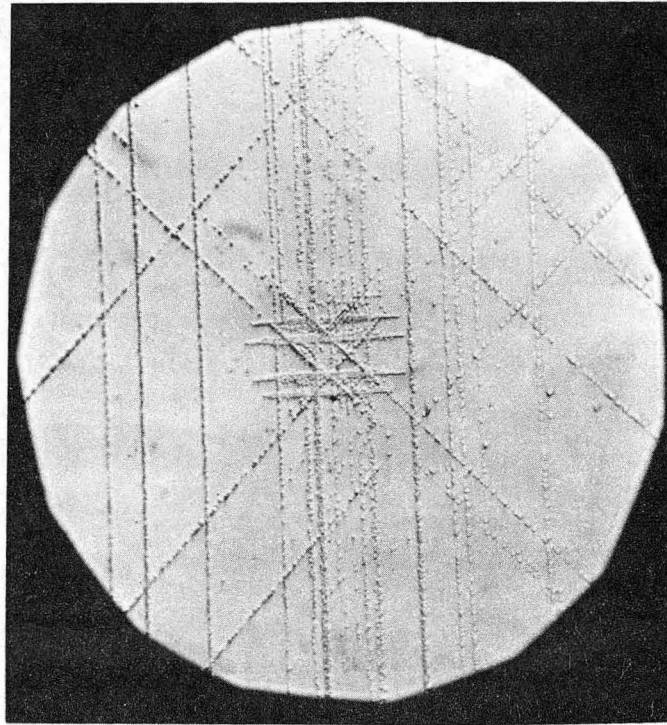
100μ

ZN-3169

Fig. 5. Rosette of "fresh" dislocations which have initiated
slip bands during deformation.

$1/4\mu$

ZN-3153

Fig. 6. Dense dislocation substructure on 45° planes in
a sample deformed at -196°C.

1/2 μ
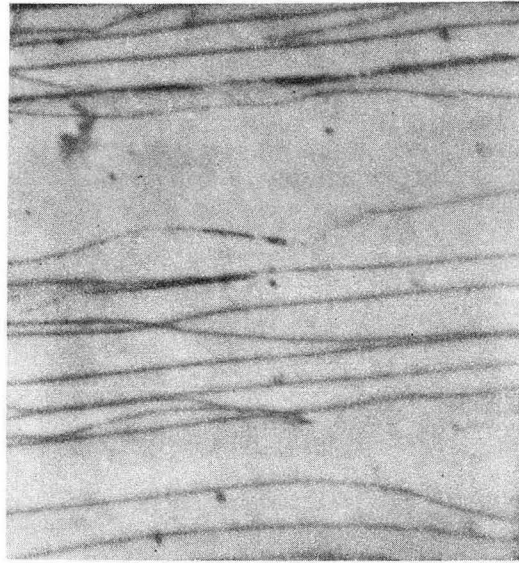
1/4 μ

ZN-3204

Figs. 7a and 7b. Dislocations on 45° slip bands in
sample deformed at 750°C.

1/4 µ
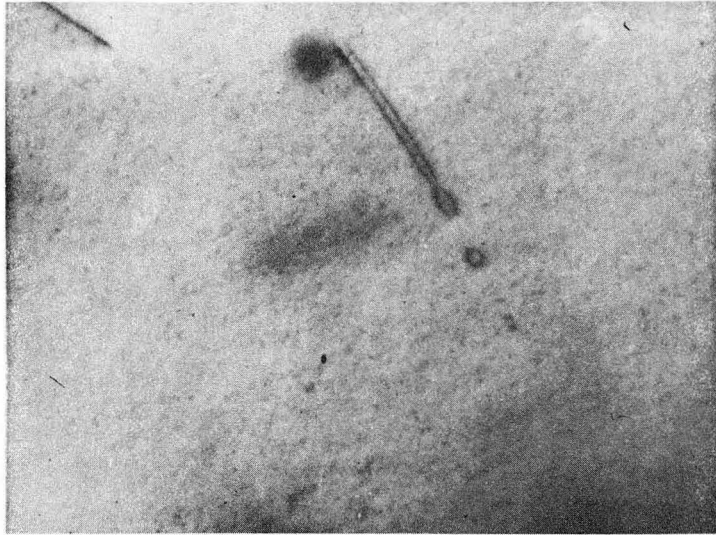
ZN-3157

Fig. 8.   Individual dislocation pair showing the pinching
off of prismatic loops.   Sample deformed at 1000°C.

30 μ
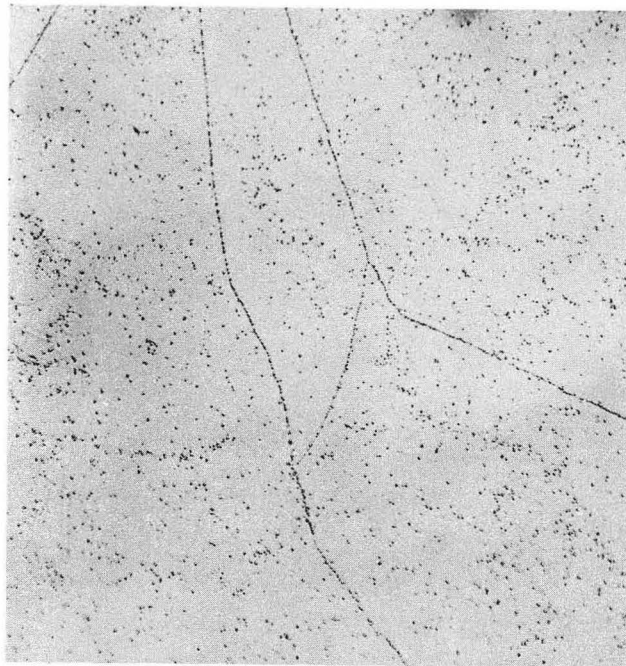
ZN-3160

Fig. 9. As received MgO crystal showing grown
in dislocation density and subgrain boundaries.
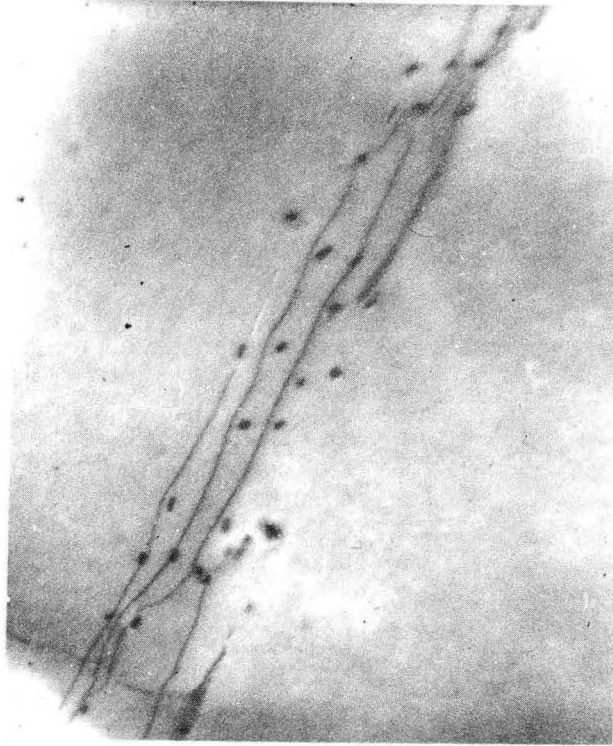
1/4 μ

ZN-3159

Fig. 10. Grown in dislocations in a tilt boundary.
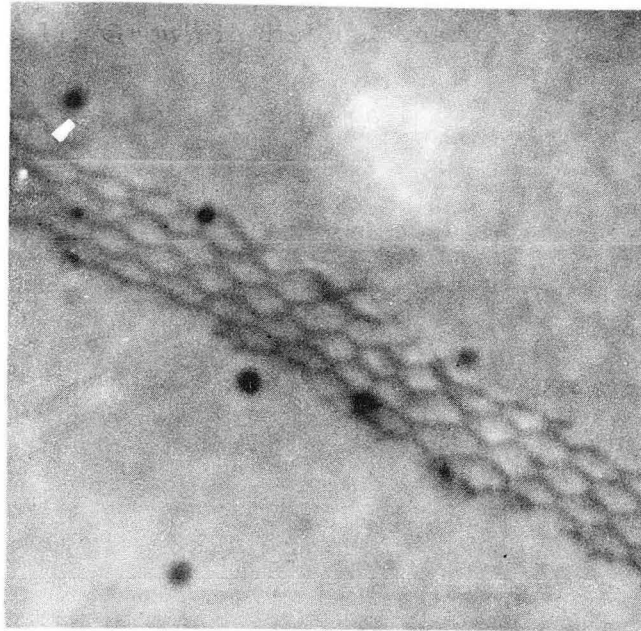
1/5μ

ZN-3155

Fig. 11. Grown in dislocations in twist boundary.
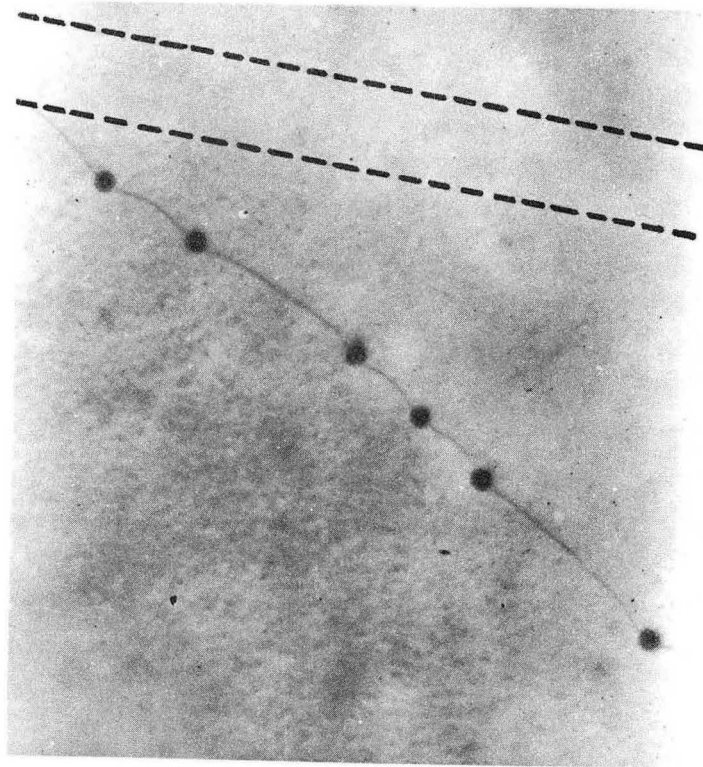
ZN-3161

Fig.12. Grown in dislocation with impurity precipitate.
The dislocation is immobile because it does not lie
on a slip plane. Dotted lines show approximately
the projection of a {110} plane.

1/4 μ
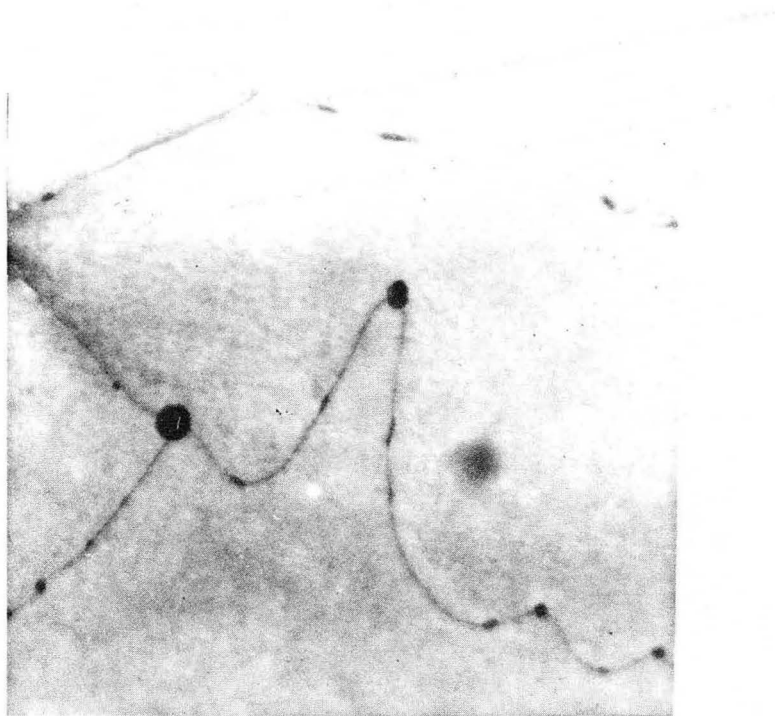
ZN-3154

Fig. 13. Grown in dislocations with a large precipitate
at a dislocation node.

1/4 μ
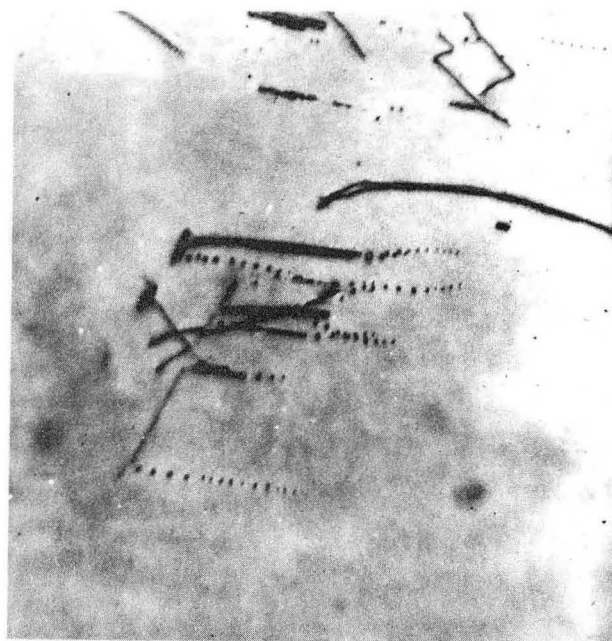
ZN-3156

Fig. 14. Dislocation pairs formed at grown in dislocations.
Smaller pairs have broken up into prismatic loops.
Sample deformed at 1200°C.

1/4 μ
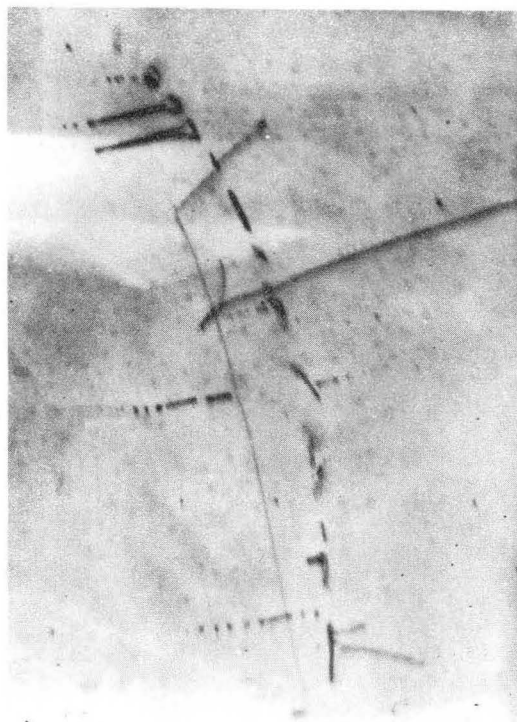
ZN-3158

Fig. 15. Dislocation pairs formed at grown in dislocations.
Smaller pairs have broken up into prismatic loops.
Sample deformed at 1200°C.

1/2 μ

ZN-3166

Fig. 16. Dislocation pairs and dislocation debris formed
at a grown in dislocation and impurity precipitates.
Smaller pairs have broken up into prismatic loops.
Sample deformed at 1000°C.

1/4 μ
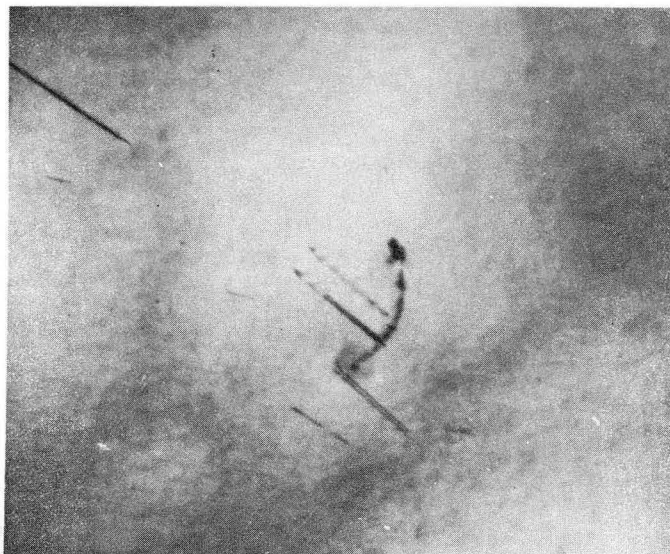
ZN-3165

Fig. 17. Dislocation pairs formed at a grown in dislocation.
Some pairs deviate from a $\langle 110 \rangle$ direction.

1/3μ

ZN-3162

Fig. 18. Dislocation pairs formed at a grown in dislocation
    in 90° slip bands.

1/4 μ
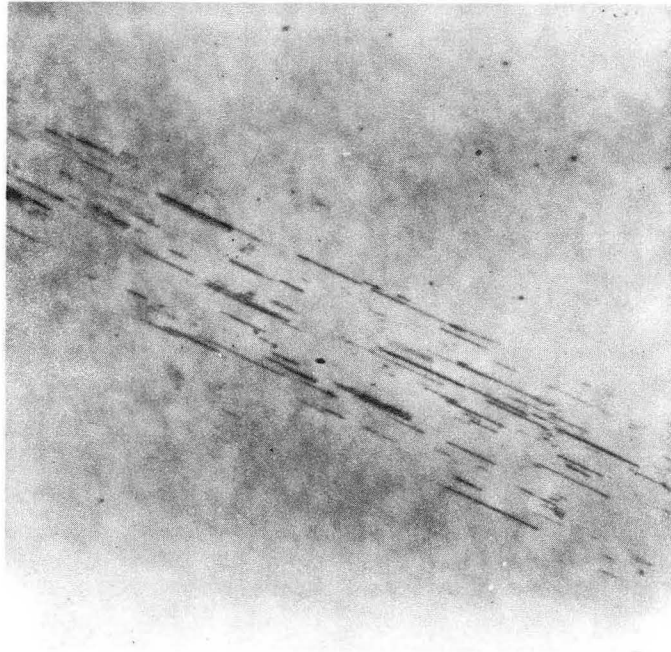
ZN-3167

Fig. 19. 90° slip band in sample deformed at -196°C.
Dislocations and pairs are aligned in ⟨110⟩ direction.
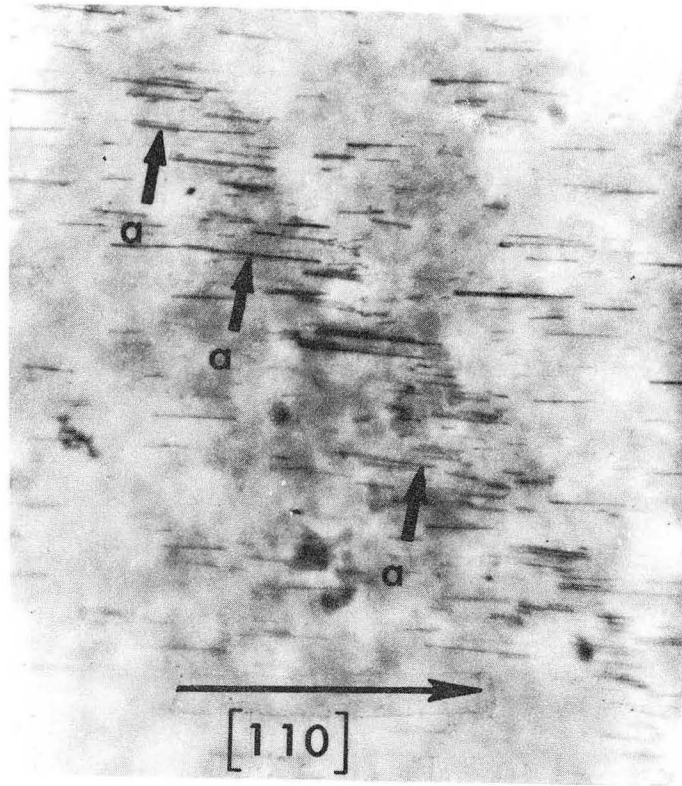
1/4 μ

ZN-3164

Fig. 20. 90° slip band in sample deformed at room
temperature. Arrows locate dislocations which
deviate from ⟨110⟩ alignment.

(a)

⊔_⊔
1/4 μ
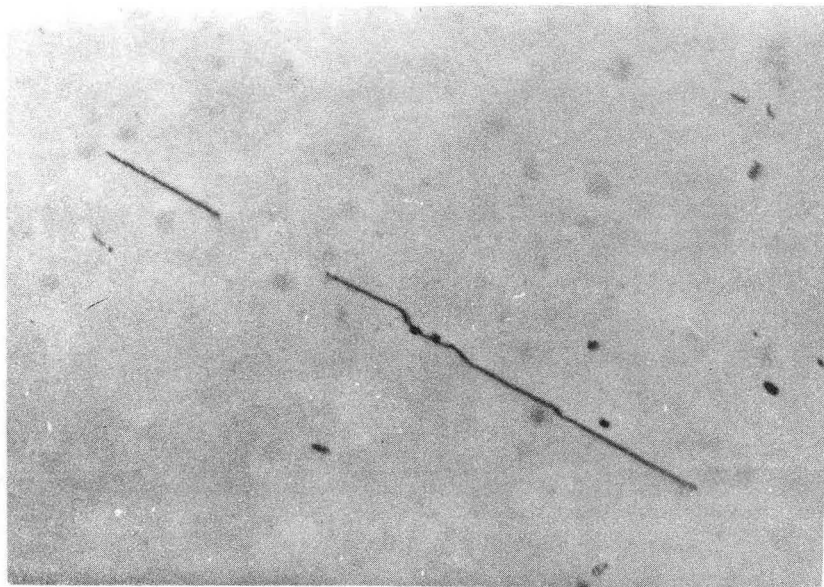
ZN-3207

Fig. 21a. Large jogs on dislocation in sample
deformed at 1300°C.

(b)

$1/4\mu$
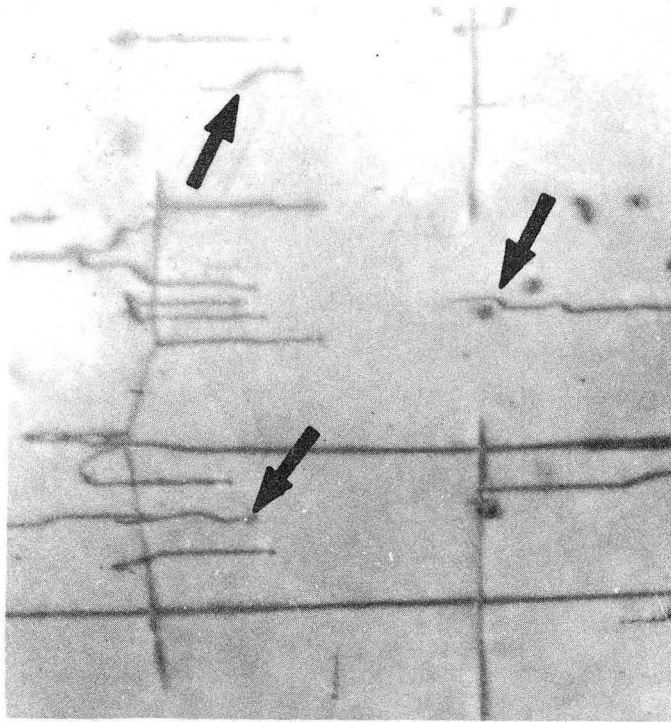
ZN-3209

Fig. 21b. Arrows locate dislocations containing jogs.
Sample deformed at 1300°C.

(a)

⊢——⊣
1/4 μ
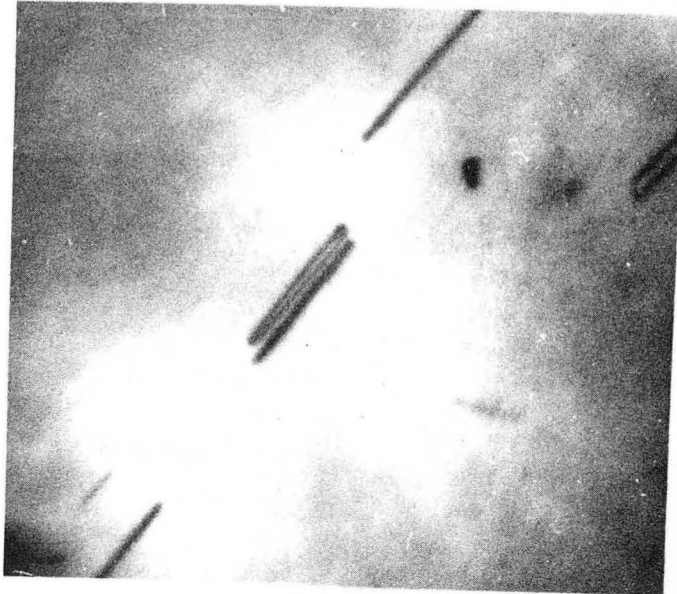
ZN-3208

Fig. 22a. Widest pair found in a sample deformed at
room temperature at a stress of 7kg/mm^2. Measured
pair separation is 250Å. Calculated maximum pair
separation for this stress is 370Å.
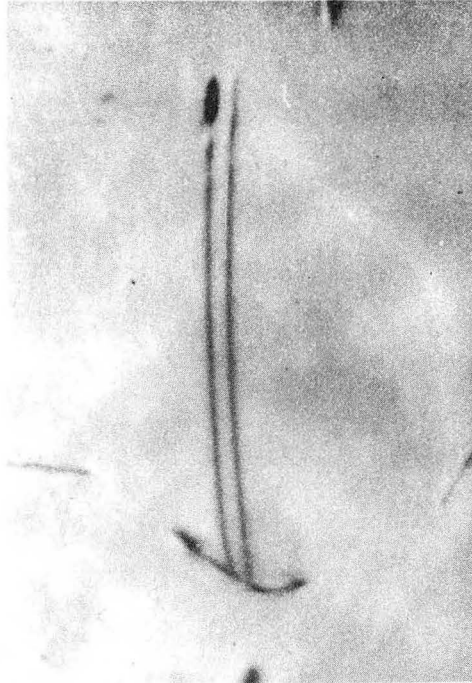
(b)

$\vdash\!\!\!\!\dashv$

$1/4\mu$

ZN-3206

Fig. 22b. Widest pair found in a sample deformed at 500°C at a stress of 3kg/mm². Measured pair separation is 600Å. Calculated maximum separation for this stress is 870 Å.